UNCERTAINTY QUANTIFICATION OF PERFORMANCE PARAMETERS IN A SMALL SCALE ORC TEST RIG

Michele Bianchi[1], Lisa Branchini[1], Nicola Casari[2], Andrea De Pascale[1], Ettore Fadiga[2], Francesco Melino[1], Saverio Ottaviano[1], Antonio Peretto[1], Michele Pinelli[2], Pier Ruggero Spina[2], Alessio Suman[2] *

[1]University of Bologna, Department of Industrial Engineering, Bologna, Italy

[2]University of Ferrara, Department of Engineering, Ferrara, Italy

* Corresponding Author

ABSTRACT

Thermodynamic measurements are affected by a certain level of uncertainty due to the sensor/probe characteristics, installation, calibration procedure, and references. In power cycle for energy production, such as standard Rankine cycles and Organic Rankine Cycles (ORC), pressure, temperature, and mass flow rate are used as the basis for estimating the cycle performance, as well as, they are used for monitoring the entire cycle and its operating conditions. In the present work, a small-scale ORC system is taken as reference for performing the assessment of the uncertainty sources and their propagation in the estimation of the cycle performance. The analysis is referred to an ORC system that operates with a temperature of the hot source lower than 100 °C, a net electric power at the generator lower than 1 kW and the R134a as the working fluid. Since the accuracy of the performance estimation is related to the performance of measurement system and to its calibration, three different scenarios have been analyzed in relation to the sensor/probe performance, calibration process, and acquisition devices' operating conditions. For the performance uncertainty estimation, temperature, pressure, and mass flow rate measurement uncertainties are taken into consideration, as well as the effect of the thermodynamic library used for calculating enthalpy values. The uncertainty values of performance parameters that characterize an ORC system such as expander work, expander power, and overall system efficiency have been assessed showing how the calibration process represents the mandatory step in the way of reducing the uncertainty band. Acquisition module and calibrator performance have to be assessed in comparison with the performance of the sensors and probes installed in the ORC system.

1. INTRODUCTION

Starting from the former idea in 1823 by Sir Humphrey Davy (Hartley, 1960) ORC systems are known as an interesting strategy to recover energy from energy waste at very low temperature. Despite their effectiveness in energy recovery, the ORC system is characterized by low-efficiency values, especially in the case when the net electric power is less than 10 kWe (Macchi and Astolfi, 2016).

Over the years several applications have been developed (Landelle et al., 2017) collecting a huge amount of data related to the performance of different expander devices, pumping systems, and heat exchanger technology. Since these applications have been compared by means of their performance, a proper assessment of the methodology/instrumentation used in common measuring systems is suggested. In common practice, the system performance calculation (e.g. thermal and electric power, efficiency, etc.) relies on the estimation of the enthalpy and, due to this, the uncertainties that characterize the elemental variables, such as pressure, and temperature, are propagated through the Equations of State (EoS), either evaluated by means of thermophysical libraries or by dedicated analytical equations (such as Redlich-Kwong, Peng-Robinson, or others as reported by Frutiger et al. 2017). Therefore, the uncertainties of the measurement chains of temperature and pressure are propagated through the library and/or EoS as a function of the ORC operating point.

In this work, the uncertainties associated to the measures of pressure and temperature, are propagated into the enthalpies through the Helmholtz equation of state of R134a implemented in CoolProp library. Subsequently, it has been assessed how these uncertainties (as absolute and relative values), together

with other contributions such as mass flow rate, affect the estimation of the most important parameters that characterize ORC systems (such as heat power input, efficiency, expander work, and power). In common installations, the ORC cycle performance is usually obtained by measuring the power output (in terms of electric power and/or torque) together with the heat power input and output. However, in this case, the uncertainty estimation process is devoted to discovering the mutual interaction among the thermodynamic variables of the ORC cycle. Taking into consideration only the thermodynamic variables related to the ORC side, it is possible to show how the proper design and operation of the measurement systems could reflect in a better performance estimation and, in turn, in a better cycle operation.
With the reference of the ORC cycle reported by Bianchi et al., 2019, four operating points are considered as a function of the temperature at the evaporator and on the mass flow rate provided by the pump. With the aim of analyzing the different level of accuracy and measurement system performance, three different levels of accuracy have been considered. The basic approach that is characterized by the off-the-shelf accuracy of the sensor, probes and acquisition module, is compared to two cases for which a calibration process is done, with the use of specific calibrator and standard procedures.

2. SMALL-SCALE ORC SYSTEM

The ORC system taken as a reference is described in details in Bianchi et al. (2019). The prototypal micro-ORC energy system was specifically designed for on-field operation but at the same time, it was equipped with several additional sensors/probes in order to detect its operating points and performance. The ORC system is based on a recuperative configuration and it currently operates with R134a as working fluid. The ORC main components are the following: (i) a brazed plate heat exchanger with 64 plates as evaporator, (ii) a brazed plate heat exchanger with 19 plates as recuperator, (iii) a shell and tube heat exchanger as condenser, (iv) a volumetric three pistons radial engine used as expander, and finally, (v) a volumetric gear pump controlled by an inverter that supplies the organic fluid over the ORC system. The water temperature at the ORC evaporator (thermal input) is controlled by means of a three-way valve installed across the closed loop responsible of the mixing process between the water at the evaporator inlet with the return water. A detailed characterization of the present ORC system is reported in Bianchi et al. (2019). Starting from the data reported in their paper, four stable operating conditions have been considered for performing the uncertainty evaluation of the measurement system, according to three different aforementioned scenarios (off-the-shelf, on-field and lab-scale calibration). The operating conditions are listed in Table 1 and they are referred to three different temperature values of the heat input. In addition, for the middle-temperature value of the heat source, two different conditions have been considered according to the different value of the mass flow rate (Case B and BB). The uncertainty assessment will be carried out for four fundamentals performance indexes, usually used for describing an ORC system. The considered indexes and their definition are listed below. According to the system layout reported in Table 1, the power heat exchanged at the evaporator is defined as

$$Q = M \cdot (h_2 - h_9) \tag{1}$$

where M is the organic fluid mass flow rate and the enthalpy values are those measured at the inlet (h_9) and the outlet (h_2) sections of the evaporator. The expander power output is defined as

$$P = M \cdot W \tag{2}$$

where the term W is calculated by means of the enthalpy difference across the expander

$$W = h_2 - h_3 \tag{3}$$

Finally, the efficiency is calculated with the ratio of the expander power output and the thermal input

$$\eta = P/Q \tag{4}$$

This efficiency value is based on the ORC thermodynamic cycle and it does not take into account the mechanical losses nor the electric generator efficiency. It is also a gross efficiency since the feed pump consumption is not included.

Table 1: Operating conditions used for the uncertainty assessment. Measurement points are numbered according to Bianchi et al., 2019

X	A	B	C	BB
p_2 [bar]	14.3	14.4	14.1	16.9
T_2 [°C]	64.6	73.8	86.0	73.6
p_3 [bar]	6.16	6.09	6.05	6.39
T_3 [°C]	41.7	51.2	63.8	47.6
p_9 [bar]	14.3	14.4	14.1	16.9
T_9 [°C]	34.5	40.4	47.9	38.6
M [kg/s]	0.10	0.10	0.09	0.14

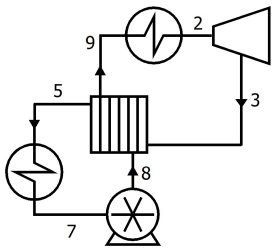

3. MEASUREMENT CHAINS AND UNCERTAINTY ASSESSMENT

In order to collect data on the operation of the system, the test bench has been instrumented with a mass flow rate measurement and some additional temperature probes and pressure sensors. The measurement equipment was realized with the aim to characterize every single component following the common procedure adopted for lab-scale ORC systems (see for examples the data collection reported by Landelle et al., 2017). For this reason, in the present work, the assessment of the measurement performance according to the different level of accuracy/calibration quality can be carried out.

The measurements of R134a temperature are made through 8 T-type thermocouples with a mineral insulating sheath, while R134a pressure is measured by ceramics pressure transducers (Honeywell FP2000 model) with a measuring range of (0 – 10) bar for the low-pressure line, and (0 – 30) bar for the high-pressure line. Temperature probes and pressure transducers are installed in the same taps using a tee fitting. Firstly, measurement taps were checked to ascertain the absence of burrs or slag and, thus, avoiding their contributions to the total error of pressure measurements, which can be remarkable (Franklin and Wallace, 1970). In each measurement point, the thermocouple (100-mm long, 1.5-mm diameter) was inserted such as allowing the evaluation of the flow temperature in the center of the pipe section. This set-up ensures the best and fast response as possible, avoiding the drawbacks peculiar of wall-mounting temperature probes, which are characterized by several uncertainties such as insulation and conduction issues, delay, and coupling with the environment. In the 90°-port of the tee, the pressure transducer is installed allowing the evaluation of pressure value in the same section of the temperature probe. This feature eliminates the uncertainty in enthalpy calculation which can derive from a different location of pressure and temperature sensors. Finally, a Coriolis flowmeter (Endress+Hauser Promass 80E model) was used to acquire the mass flow rate. This device is located between the receiver and pump. The measuring range is (0 – 1) kg/s.

All acquired signals are transmitted to a desktop by a National Instrument FPGA device (CompactRIO). In particular, the NI 9213 acquisition module reads the voltage thermocouples signals, while the NI 9201 and NI 9203 (voltage and current acquisition modules) elaborate the signals from the mass flow and pressure sensors, respectively. These devices are comprised in the uncertainty assessment.

In addition, a microcontroller implements the data processing through the aid of the thermodynamic library CoolProp (Bell et al., 2014), which is integrated into the software and allows the obtainment of the enthalpy values as a function of temperature and pressure measured values. Since the Coolprop library accuracy affects the calculation of the enthalpy, this has been considered also in the evaluation of the enthalpy uncertainty by means of a specific procedure reported in the following paragraph.

Table 2 reports the Component Off-the-Shelf (COTS) characteristic and uncertainty that refers to the instrument accuracy as indicated on the data sheet. These data represent a reference for the probe/sensor selection, and, in the case of a design-stage uncertainty assessment (in the present work named off-the-shelf uncertainty assessment) they are assumed as representative values for the measurement performance of each device/acquisition module. In the case of a calibration process that involves the entire measurement chain, these values are replaced by different values, which allow the obtainment of different uncertainty values. These different approaches are described in the following sections.

3.1 Uncertainty calculation

The uncertainty calculation of the ORC performance parameters is based on the procedure reported in the standard ISO/IEC Guide 98 and EA-4/02M. The propagation of the uncertainty is realized by means of the classic procedure based on propagation rule. According to the ORC performances parameters,

Table 2: Operating conditions used for the uncertainty assessment

Sensor	Output signal	COTS	Acquisition module
T-type thermocouple	± 80 mV	±0.5 °C	NI 9213
Pressure transducer	(0 – 5) V	±0.25 % FS	NI 9201
Coriolis mass flow meter	(4 – 20) mA	±0.30 % RV	NI 9203

the uncertainty of the power thermal input Q, expander power output P, expander thermodynamic work W, and efficiency η can be expressed as follows:

$$\delta Q = \sqrt{\left(\frac{\partial Q}{\partial M}\right)^2 \delta M^2 + \left(\frac{\partial Q}{\partial h_2}\right)^2 \delta {h_2}^2 + \left(\frac{\partial Q}{\partial h_3}\right)^2 \delta {h_3}^2} \quad (5)$$

$$\delta P = \sqrt{\left(\frac{\partial P}{\partial M}\right)^2 \delta M^2 + \left(\frac{\partial P}{\partial W}\right)^2 \delta W^2} \quad (6)$$

$$\delta W = \sqrt{\left(\frac{\partial W}{\partial h_2}\right)^2 \delta {h_2}^2 + \left(\frac{\partial W}{\partial h_3}\right)^2 \delta {h_3}^2} \quad (7)$$

$$\delta \eta = \sqrt{\left(\frac{\partial \eta}{\partial P}\right)^2 \delta P^2 + \left(\frac{\partial \eta}{\partial Q}\right)^2 \delta Q^2} \quad (8)$$

The last step is to relate the uncertainty of the enthalpy to the thermodynamic measurement of pressure and temperature

$$\delta h = \sqrt{\left(\frac{\partial h}{\partial p}\right)^2 \delta p^2 + \left(\frac{\partial h}{\partial T}\right)^2 \delta T^2} \quad (9)$$

where the first derivatives (pressure and temperature) are estimated using the CoolProp library (see for reference Thorade and Saadat, 2013). In the CoolProp implementation, the partial derivatives of the state properties with respect to temperature can be calculated directly, because the temperature is one of the independent variables (together with the density) of the Helmholtz energy EoS. By contrast, partial derivatives with respect to dependent variables (such as pressure) cannot be calculated directly. In this case, CoolProp is able to express as a combination of partial derivatives with respect to the independent variables any partial derivative with respect to arbitrary properties (Thorade and Saadat, 2013). Therefore, using the CoolProp library, the propagation of the uncertainty values related to temperature and pressure measurements can be performed. In the following paragraphs, each uncertainty contribution will be analyzed and estimated according to the three different cases considered in the present work.

3.2 Off-the-shelf uncertainty analysis

This first approach is the simplest way to manage the uncertainty in a measurement system, for that, no calibration process was carried out. The uncertainty assessment is based on the data reported in each data sheet of probes/sensors and acquisition module as delivered by the manufacturer (off-the-shelf). The uncertainty values of mass flow rate, temperature and pressure are estimated taking into consideration all components of the measurement chains.

The mass flow rate is measured by means of a Coriolis flow meter and its analog signal (4 – 20) mA is acquired by the acquisition module NI 9203. This acquisition module is characterized by two different uncertainty contributions related to the gain and to the offset. These values are reported in the datasheet as the uncalibrated condition in the presence of greater temperature variation (comprises in the range of -40 °C – 70 °C). The gain uncertainty $U_{M,gain}$ is equal to ±0.66 % of the reading value (RV) while, the offset uncertainty $U_{M,offset}$ is equal to ±0.54 % of the full-scale (FS) (equal to 21.5 mA in the present case). Since these uncertainty sources are assumed as equally distributed over the measurement range, they are considered to have a rectangular probability distribution. This implies that the present values have to be divided by $3^{1/2}$ for calculating the standard deviation equivalents. Given this description, three terms have to be combined for calculating the uncertainty value of the mass flow rate

$$\delta M = \sqrt{\left(\frac{U_{c,s}}{\sqrt{3}}\right)^2 + \left(\frac{U_{M,gain}}{\sqrt{3}}\right)^2 + \left(\frac{U_{M,offset}}{\sqrt{3}}\right)^2} \quad (10)$$

where $U_{c,s}$ is the COTS uncertainty of the Coriolis sensor (see Table 2), which is considered equally distributed over the measurement range (in a similar way, it is divided by $3^{1/2}$ for calculating the standard deviation equivalents). Since the calibration process of the mass flow rate meter is realized by the manufacturer, in the present investigation, the estimation of δM reported in Eq. (10) is used for all the three considered cases (COTS, on-field and lab-scale calibrated). As reported in Casari et al. (2019), the CFM operation could be affected by pressure pulsations generated by the gear pump. Pump cavitation, evaporator and condenser temperature values, and gear pump speed determine the magnitude of the pressure pulsation, and in turn, the interaction between pump and CFM. However, in the present work, no additional uncertainty terms are considered related the installation in order to show the influence of thermodynamic properties and their evaluation on ORC performance parameters.
The temperature is measured by means of T-type thermocouples, and their analogic signal is acquired by the acquisition module NI 9213. This acquisition module is characterized by an overall uncertainty value $U_{t,module}$ equal to ±1 K in the temperature range considered in the present analysis (298 – 373) K. This estimation accounts for uncertainty sources related to gain, offset, nonlinearity, and cold-junction compensation. This uncertainty is assumed as equally distributed over the measurement range, and in a similar way to the previous case, it is considered to have a rectangular probability distribution. In this case, only two terms are combined for calculating the uncertainty value of the temperature, that is

$$\delta T_{\mathrm{COTS}} = \sqrt{\left(\frac{U_{\mathrm{t,s}}}{\sqrt{3}}\right)^2 + \left(\frac{U_{\mathrm{t,module}}}{\sqrt{3}}\right)^2} \tag{11}$$

where U_t is the COTS uncertainty of the temperature probe (see Table 2), which is considered equally distributed over the measurement range.
The pressure is measured by means of pressure transducers and their analog signal (0 – 5) V is acquired by the acquisition module NI 9201. Similarly to the previous case, this acquisition module is characterized by gain and offset sources of uncertainties. These values are reported in the datasheet as the uncalibrated condition in the presence of greater temperature variation (comprises in the range of -40 °C – 70 °C). The gain uncertainty $U_{p,gain}$ is equal to ±0.67 % RV while, the offset uncertainty $U_{p,offset}$ is equal to ±1.25 % FS (equal to 10.53 V in the present case). Similarly, these uncertainty sources are assumed as equally distributed over the measurement range. Hence

$$\delta p_{\mathrm{COTS}} = \sqrt{\left(\frac{U_{\mathrm{p,s}}}{\sqrt{3}}\right)^2 + \left(\frac{U_{\mathrm{p,gain}}}{\sqrt{3}}\right)^2 + \left(\frac{U_{\mathrm{p,offset}}}{\sqrt{3}}\right)^2} \tag{12}$$

where $U_{p,s}$ is the COTS uncertainty of the pressure transducer (see Table 2), which is considered equally distributed over the measurement range.

3.3 Field-calibrated uncertainty analysis

In this second approach, pressure sensors and temperature probes are calibrated on-field by means of a standard procedure. A standard procedure consists in the definition of the first order (linear) calibration curve realized using several pairs of measured pressure and reference pressure values. The Best Straight Line (BSL) was obtained by considering a minimum of 25 independent points and it is used during the tests to correct the measured pressure values. The on-field calibration process is usually carried out without a detailed evaluation of the sensor/probe hysteresis due to the impossibility to control the stability of the output signal. In addition, this type of calibration implies the impossibility to eliminate signal noise and to control the environmental conditions which is one of the major issue involved in the pressure measurement. Beyond these limitations, the on-field calibration process was performed with specific calibrators devices, described as follows.
Each pressure sensor with its correspondent acquisition device has been individually calibrated using a pressure calibrator MicroCal PM200+, representing the in-house laboratory secondary standard which, in turn, is calibrated towards a primary laboratory standard certified in agreement with the Italian Accreditation Body (Accredia). After this procedure, the type B uncertainty is obtained by considering the uncertainty of the primary laboratory standard (that represents the reference uncertainty of the certified laboratory standard) $U_{p,PLS}$ (considered as a Gaussian distribution, and for this reason it is dived by 2 for calculating the standard deviation equivalents) and the residual uncertainty value of the pressure measurement chain $E_{p,R}$. The latter value is estimated considering the peak-to-valley amplitude of a set of pressure values obtained during 10 minutes of constant pressure input (generated and controlled by

the MicroCal PM200+) and it is considered to have a rectangular probability distribution. This procedure also allows the evaluation of the type A uncertainty by estimating the standard deviation (considered as a Gaussian distribution, and for this reason, it is dived by 2 for calculating the standard deviation equivalents) of the set of data $U_{p,\sigma}$. The size of the sample (about 600 pressure measurements) ensures the proper application of the statistic methodology. The final assessment of the pressure measurements uncertainty is

$$\delta p_{field} = \sqrt{\left(\frac{U_{\mathrm{p,PLS}}}{2}\right)^2 + \left(\frac{E_{\mathrm{p,R}}}{\sqrt{3}}\right)^2 + \left(\frac{U_{\mathrm{p},\sigma}}{2}\right)^2} \tag{13}$$

A similar procedure is applied to the temperature sensors. The thermocouples are calibrated in a thermostatic static furnace (Isotech Jupiter 650) that introduces an estimated error of $E_{\mathrm{T,F}}$ equal to 0.10 K (related to the non-ideal uniform temperature of the bath) and a first order (linear) calibration curve was obtained in the range of (288 – 365) K. The reference temperature was obtained with a Pt100 Class A thermistor (4-wire) coupled with the Microcal 200+ calibrator. This reference temperature chain represents the in-house laboratory secondary standard calibrated towards a primary laboratory standard certified in agreement with the Italian Accreditation Body (Accredia), characterized by an uncertainty equal to $U_{\mathrm{T,PLS}}$ = 0.09 K. Type A and Type B uncertainty contributions are established by means of a similar procedure used for pressure sensors. The on-field calibration does not allow the proper control of the environmental conditions, and, the variability encountered in the ambient temperature could affect the calibration process (variation of ice-point reference, and thermocouple signal noise). Finally, the uncertainty related to the installation and radiation effects (Benedict, 1984) was neglected considering the similar temperature between the duct walls and the tip of the thermocouple. Therefore

$$\delta T_{field} = \sqrt{\left(\frac{U_{\mathrm{T,PLS}}}{2}\right)^2 + \left(\frac{E_{\mathrm{T,F}}}{\sqrt{3}}\right)^2 + \left(\frac{E_{\mathrm{T,R}}}{\sqrt{3}}\right)^2 + \left(\frac{U_{\mathrm{T},\sigma}}{2}\right)^2} \tag{14}$$

3.4 Lab-scale uncertainty analysis

In this last approach, pressure sensor and temperature probes are calibrated by means of a standard procedure in a controlled (lab-scale) conditions. A similar procedure of the previous case was adopted in order to define the BSL for each pressure and temperature measurements. The lab-scale procedure allows the evaluation of the hysteresis by means of a two-way calibration process (from lower to higher-pressure values, and vice-versa). Since the calibration process was carried out in the same conditions as the ORC system operation, the temperature effects on the pressure measurement were considered intrinsically. Analogous consideration can be done for the ice-point reference value that will be included in the calibration process. The overall uncertainty value of pressure δp_{lab} and temperature δT_{lab} measurements are estimated by Eqs 13, and 14, respectively.

4. COMPARISONS

In this final part of the present work, several guidelines are reported with the aim to focus the attention to the major uncertainty contributions on the estimation process of the ORC performance. The present section is divided according to two different analyses. The first one involves the analysis of the single contributor to the measurement chains of pressure and temperature, while the second one is focused on the uncertainty contributions on the ORC performance uncertainty. Before these two detailed analyses, some considerations about the uncertainty assessment of the considered cases are reported. The Tables 3 – 5 report the ORC performance and the associated uncertainty value for the off-the-shelf, on-field and lab-scale calibrated cases, respectively. For the sake of completeness, in the tables, together with the absolute values of the uncertainty δ, the percentage values are also reported. From the values reported in the tables, clearly visible is the reduction of the uncertainty percentage values moving from the coldest to the hottest temperature at the evaporator, for all the considered performance indexes. The COTS case shows the highest uncertainty values for all the ORC performances, demonstrating how the calibration process is required for reducing the magnitude of the uncertainty value.

A graphic representation of the uncertainty values of the expander power and the ORC efficiency, according to the case and for the four operating conditions, is reported in Figure 1. The uncertainty of the ORC efficiency (Fig. 1b) appears more affected by the calibration process. As shown, the trend of COTS, on-field, and lab-scale calibrated are more dispersed than to the trends of ORC power (Fig. 1a).

Table 3: ORC performance and the associated uncertainty value for the off-the-shelf case. Uncertainty values δ are reported between brackets while percentage values are reported a side

	A		B		C		BB	
X	**X(δ)**	**%**	**X(δ)**	**%**	**X(δ)**	**%**	**X(δ)**	**%**
Q [W]	19020 (846)	4.45	19201 (855)	4.45	17519 (861)	4.92	25829 (861)	3.33
P [W]	836 (105)	12.59	942 (116)	12.32	1010 (99)	9.77	1179 (143)	12.09
W [J/kg]	8360 (986)	11.79	9420 (1084)	11.51	11220 (950)	8.47	8670 (1009)	11.64
η [-]	0.044 (0.0059)	13.35	0.049 (0.0064)	13.10	0.058 (0.0063)	10.94	0.046 (0.0057)	12.54

Table 4: ORC performance and the associated uncertainty value for the on-field calibration case. Uncertainty values δ are reported between brackets while percentage values are reported a side

	A		B		C		BB	
X	**X(δ)**	**%**	**X(δ)**	**%**	**X(δ)**	**%**	**X(δ)**	**%**
Q [W]	19020 (133)	0.70	19201 (137)	0.71	17519 (131)	0.75	25829 (153)	0.59
P [W]	836 (53)	6.38	942 (59)	6.22	1010 (47)	4.61	1179 (74)	6.28
W [J/kg]	8360 (531)	6.35	9420 (583)	6.19	11220 (512)	4.56	8670 (543)	6.27
η [-]	0.044 (0.0028)	6.42	0.049 (0.0031)	6.26	0.058 (0.0027)	4.67	0.046 (0.0029)	6.31

Table 5: ORC performance and the associated uncertainty value for the lab-scale calibration case. Uncertainty values δ are reported between brackets while percentage values are reported a side

	A		B		C		BB	
X	**X(δ)**	**%**	**X(δ)**	**%**	**X(δ)**	**%**	**X(δ)**	**%**
Q [W]	19020 (50)	0.26	19201 (51)	0.27	17519 (48)	0.28	25829 (62)	0.24
P [W]	836 (15)	1.82	942 (17)	1.78	1010 (13)	1.32	1179 (21)	1.79
W [J/kg]	8360 (150)	1.80	9420 (166)	1.77	11220 (145)	1.29	8670 (154)	1.78
η [-]	0.044 (0.0008)	1.84	0.049 (0.0009)	1.80	0.058 (0.0008)	1.34	0.046 (0.0008)	1.81

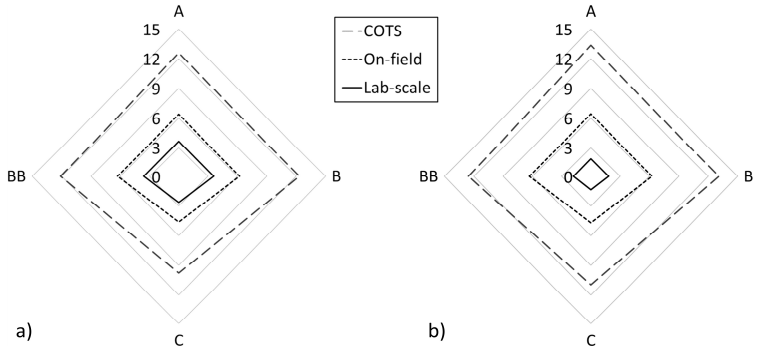

Figure 1: Uncertainty percentage values of a) ORC power and b) ORC efficiency for the four operating points divided according to the uncertainty assessment scenario

Moving from the off-the-shelf uncertainty assessment to the cases for which a calibration process is done, the uncertainty is reduced by an order of magnitude. In particular, from the worst to the best scenario (beyond the cases related to the hot source temperature) the uncertainty value of ORC power is reduced from 12.59 % to 1.32 %, while the uncertainty of ORC efficiency is reduced from 13.35 % to 1.34 %.

4.1 Contributors to the measurement chain uncertainty

In this first section, the analysis of the uncertainty contribution to measurement chain of temperature and pressure is reported. Based on Eqs 11 – 14, Figs. 2 – 4 report the percentage values of the contributions to the uncertainty of temperature and pressure measurement chains estimated for the COTS, on-field, and lab-scale calibrated cases. These data are referred to the case with the middle temperature at the evaporator (Case B, see Table 1), and it is representative of the four operating points. For the COTS case (reported in Fig. 2) the main contribution to the uncertainty of temperature and

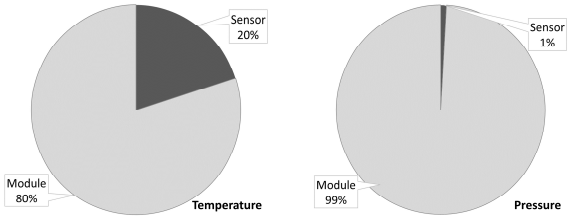

Figure 2: Uncertainty contributions of temperature and pressure measurement chain (COTS case)

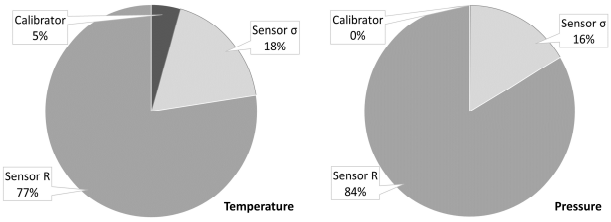

Figure 3: Uncertainty contributions of temperature and pressure measurement chain (on-filed calibration case)

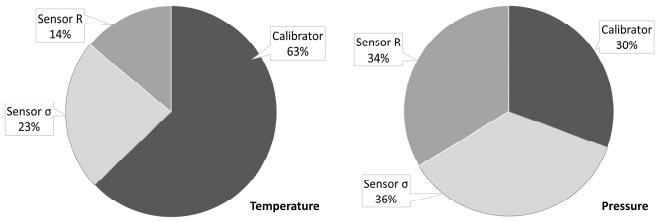

Figure 4: Uncertainty contributions of temperature and pressure measurement chain (lab-scale calibration case)

pressure is represented by the acquisition module measurement performance that is responsible for the 80 % and 99 % of the overall uncertainty value for temperature and pressure respectively. In this case, the proper solution for improving the measurement performance is based on the improvement of the acquisition module capabilities, especially for the pressure measurement.

Moving to the cases for which the calibration process is carried out, the scenario changes. Sensor/probe performance affect the uncertainty by the most in the case of on-field calibration (see Fig. 3), due to the presence of uncontrolled condition and effects of environment condition, noise and signal disturbance. In that case, the adoption of an electromagnetic shielding could improve accuracy.

For the lab-scale calibration process (reported in Fig. 4), the performance and the accuracy of the calibrator represent the most relevant contribution for the temperature probe calibration process. The proper selection of the in-house laboratory secondary standard as well as the primary laboratory standard has comparable importance to the probe selection. The temperature chains calibration process is affected by the uncertainty due to the uniformity of the bath that is comparable (and sometimes is higher) to the uncertainty of the calibrator. For the pressure measurement chains, calibrator and sensor characteristics play a similar role in the uncertainty assessment.

Finally, the analysis of the mass flow rate measurement chains is reported. Mass flow rate uncertainty is affected by the acquisition module performance by 99.8 %. Coriolis mass flow meter is an expensive and very accurate device but, in common application, the acquisition module lowers the performance of the mass flow rate measurement chains by order of magnitude.

4.2 Contributors to the ORC performance uncertainty

The second and last analysis is carried out in a similar manner to the previous one, but in this case, the contributions are referred to the ORC system performance. With the reference of Eqs. 5 – 8, Figs. 5, and 6 report the percentage values of the contributions to the uncertainty of power thermal input Q, expander power output P, expander thermodynamic work W, and efficiency η estimated for the COTS, and lab-scale calibrated cases. These data are referred to the case with the middle temperature at the evaporator (Case B, see Table 1), and it is representative of the four operating points.

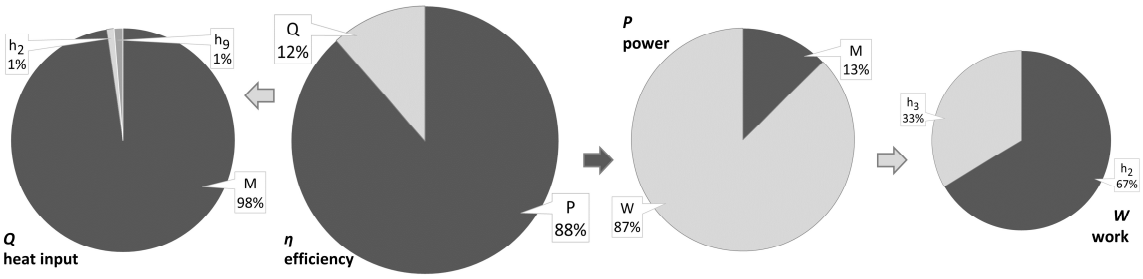

Figure 5: Contributions to the uncertainty values of ORC efficiency (COTS)

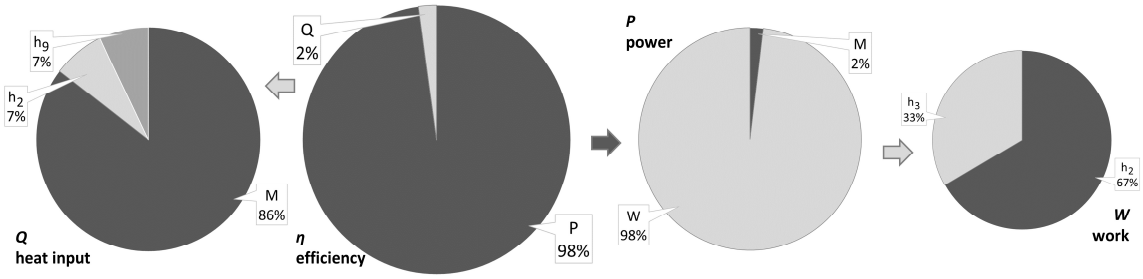

Figure 6: Contributions to the uncertainty values of ORC efficiency (lab-scale calibration case)

Figure 5 shows the contributions for the COTS case. Starting from the contributions to the efficiency uncertainty, the two terms are unpacked into their former terms. Therefore, the major contribution to the efficiency uncertainty is represented by the uncertainty of the power output that is mainly due to the uncertainty of the estimation of the thermodynamic work *W*. This latter term is affected by the uncertainty of the enthalpy estimation and in particular, to the uncertainty of the enthalpy in the lower pressure line of the ORC system. Regarding the power thermal input, this is affected by the term related to the uncertainty estimation of the mass flow rate. This fact is mainly due to the partial derivative term, that corresponds to the enthalpy difference across the evaporator. For that term, the uncertainty increases when the enthalpy difference increases.
A similar consideration can be done for the lab-scale case, reported in Fig. 6. The difference is mainly due to the fact that the acquisition module of the mass flow rate is not affected by the variation of the operating temperature, and its performance is better than in that showed in the previous case. For this reason, the percentage values of mass flow rate and enthalpy uncertainties appear different, and the uncertainty of the thermodynamic process became more detrimental.

5. CONCLUSIONS

In this paper, the uncertainty assessment of an ORC system has been performed. Three cases have been considered in relation to the quality and performance of the measuring systems. The rough-and-ready approach that consists in the evaluation of the uncertainty by means of the off-the-shelf performance of the sensors and probes, has been compared to a more accurate approach based on the calibration process. The calibration process has been carried out with two different levels of accuracy: the first one mainly related to the usual on-field condition, and the second one more related to the lab-scale condition. Differences in the control of the environment condition and noise on the analog signals of the sensors/probes represent the main differences between these two cases.
The analysis of the measurement chains of pressure and temperature has shown that, without a specific calibration process, the acquisition module could represent the major bottleneck for the uncertainty reduction process. In the case of the calibration process, the proper selection of the calibrator (especially in the case of temperature measurement chain) is fundamental for reducing the overall uncertainty value.
The ORC performance indexes, such as power and efficiency, have shown that the estimation of the thermodynamic process, especially at the lower pressure line of the system, has greater effects on the overall uncertainty values. The higher contribution is due to the estimation of power, which is affected by the enthalpy difference across the evaporator.

Based on the outcomes of the present work, the proper selection of the sensor and probes has to be propped up by the selection of the acquisition module. When the calibration process has been done, the calibrator performance and the primary laboratory standard have comparable importance of sensor and probes.

NOMENCLATURE

h	enthalpy	T	temperature
M	mass flow rate	U	uncertainty
P	expander power	W	work
p	pressure	X	variable
Q	power heat		

Subscript

c	Coriolis sensor	PLS	primary laboratory standard
COTS	component-off-the-shelf	R	residual
g	gain	s	sensor
F	furnace	t	temperature probe
field	field (calibrated on-)		
lab	lab-scale (calibrated on-)	**Greek letters**	
module	module	δ	variation (uncertainty)
offset	offset	η	efficiency
p	pressure sensor	σ	standard deviation

REFERENCES

Bell IH, Wronski J, Quoilin S, Lemort V. Pure and pseudo-pure fluid thermophysical property evaluation and the open-source thermophysical property library CoolProp. Ind. Eng. Chem. Res; vol. 53 issue 6, 2014, pp.2498–508. DOI: 10.1021/ie4033999

Benedict RP, Fundamentals of Temperature, Pressure, and Flow Measurements, third ed., John Wiley and Sons Inc, New York, USA, 1984.

Bianchi M, Branchini L, Casari N, De Pascale A, Melino F, Ottaviano , Pinelli M, Spina PR, Suman A. Experimental analysis of a micro-ORC driven by piston expander for low-grade heat recovery (2019) Applied Thermal Engineering, pp. 1278-1291. DOI: 10.1016/j.applthermaleng.2018.12.019

Casari N, Fadiga E, Pinelli M, Randi S, Suman A. Pressure Pulsation and Cavitation Phenomena in a Micro-ORC System (2019) Energies, 12. DOI:10.3390/en12112186

Franklin RE, Wallace JM. Absolute measurements of static-hole error using flush transducers (1970) J. Fluid Mech., 42 (1) pp. 33–48, https://doi.org/10.1017/ S0022112070001052

Frutiger J, Bell I, O'Connell JP, Kroenlein K, Abildskov J, Sin G. Uncertainty assessment of equations of state with application to an organic Rankine cycle (2017) Molecular Physics, 115 (9-12), pp. 1225-1244. DOI: 10.1080/00268976.2016.1275856

Hartley H. "'Sir Humphrey Davy' The Wilkins Lecture", Proc Roy Soc A (1960), 225, pp.153-180

Landelle A, Tauveron N, Haberschill P, Revellin R, Colasson S. Organic Rankine cycle design and performance comparison based on experimental database (2017) Applied Energy, 204, pp. 1172-1187. DOI: 10.1016/j.apenergy.2017.04.012

Macchi E, Astolfi M. 2016 *Organic Rankine Cycle (ORC) Power Systems* 1st Edition, Woodhead Publishing, United Kingdom, 698 pages

Thorade M, Saadat A. Partial derivatives of thermodynamic state properties for dynamic simulation (2013) Environmental Earth Sciences, 70 (8), pp. 3497-3503. DOI: 10.1007/s12665-013-2394-z

ACKNOWLEDGEMENT

The research was partially supported by the Italian Ministry of Economic Development within the framework of the Program Agreement MSE-CNR "Mi-cro co/tri generazione di Bioenergia Efficiente e Stabile (Mi-Best)".